Closed-Form Analysis of Equal-Gain Diversity in Wireless Radio Networks

Nikos C. Sagias, *Member, IEEE*

***Abstract*—This paper deals with the performance of predetection equal-gain combining (EGC) receivers operating over multipath fading plus cochannel interference (CCI) and additive white Gaussian noise channels. The desired components of the received signals are considered to experience independent but not-necessarily identically distributed Nakagami-m fading, while the interferers are subject to independent Rayleigh fading. The analysis is not only limited to equal average fading power interferers, but the case of interferers with distinct average powers is also examined. By following the coherent interference power calculation, novel closed-form expressions for the moments of the EGC output signal-to-interference-plus-noise ratio (SINR) are derived, which are being used to study the performance of the average output SINR. Furthermore, by assuming an interference-limited fading scenario, novel closed-form union performance bounds are derived. More specifically, tight upper bounds for the outage and average symbol error probability for several constant envelope modulation schemes, and lower bounds for the Shannon average spectral efficiency, are provided. Numerical results demonstrate the effect of the number of interferers, the number of the receiver branches, and the severity of fading on the EGC receiver performance. Computer simulations have been also performed to verify the tightness of the proposed bounds and the correctness of the mathematical analysis. It is shown that the performance of cellular radio systems in the uplink is degraded mainly from the first-tier CCI of the adjacent cells.**

***Index Terms*—Bit error probability (BEP), broadband wireless networks, cellular telecommunications, cochannel interference (CCI), equal-gain combining (EGC), Gaussian interference model, mobile radio, Nakagami-m fading, outage probability (OP), Shannon's capacity, spectral efficiency.**

I. Introduction

DEMANDS for increased capacity broadband cellular networks have forced the systems designers to decrease the channel reuse distances, but with this design scheme, the overall network capacity cannot be made as large as desired. The deliberate reuse of radio channels over relatively short distances limits the reception quality mainly due to cochannel interference (CCI) from the adjacent cells [1]. Additionally, the reception quality is further degraded due to the multipath propagation phenomenon and thermal noise. A well-known technique in order to mitigate the impact of fading and CCI is diversity, which is considered as an attractive means for improving the performance of cellular radio networks. Among the most popular diversity techniques, maximal-ratio combining (MRC), equal-gain combining (EGC), and selection combining (SC) are included. EGC presents a significant practical interest because it provides better performance than SC and comparable to MRC but at lower implementation complexity than the latter one [2]. By comparing the two classical implementations of EGC, referred to as predetection and postdetection combining, the former provides better performance than the latter at the expense of increased circuitry complexity, since channel phase estimation is required. In predetection EGC, the received signals in each of the N antennas are cophased with respect to the desired component, equally weighted, and summed to give the resultant output signal [3].

Several papers have been published in the open technical literature concerning the performance of predetection equal-gain diversity systems under multipath fading (see [3]–[16] and references therein), while when CCI is further being considered, a smaller number have been also published [17]–[22]. In an early work [17], the outage performance of EGC receivers under Nakagami-m fading channels and CCI has been studied. The same authors, in [18], have analytically derived the average bit error probability (ABEP) of dual-branch EGC receivers with M-ary-phase shift keying (M-PSK) signaling operating over Nakagami-m fading in the presence of Rayleigh CCI. In two other related works [19], [20], useful analytical expressions for the outage performance of EGC receivers operating in an interference-limited Rayleigh fading environment with multiple cochannel interferers have been obtained, while in [21], the EGC performance of band-limited binary-phase-shift-keying systems operating in Nakagami-m fading with CCI has been analyzed. In that paper, by employing spectrum raised-cosine and Beaulieu–Tan–Damen pulse shapes, corresponding ABEP expressions have been analytically derived. Recently, the average output signal-to-interference-plus-noise ratio (SINR) of N-branch EGC receivers over correlated nonidentically distributed Nakagami-m fading channels, in the presence of multiple CCI and additive white Gaussian noise (AWGN), has been analyzed [22]. A common point of the aforementioned papers [17]–[21] is that the derived outage and error performance formulas are either in a form of unsolved integrals with infinite limits or in a form of infinite sums where a truncation error is involved. The lack of closed-form expressions stems from the difficulty of finding a solution for the distribution of the sum of N fading envelopes. However, another well-accepted approach for evaluating the performance of such difficult problems is

Manuscript received March 1, 2005; revised September 4, 2005, December 8, 2005, and March 2, 2006. This paper was presented in part at the 12th National Conference on Communications (NCC'2006), New Delhi, India, January 2006. The review of this paper was coordinated by Dr. A. Chockalingam.

The author was with Laboratory of Electronics, Department of Physics, University of Athens, Zografou, GR-15784 Athens, Greece. He is now with the Institute of Informatics and Telecommunications, National Centre for Scientific Research—"Demokritos," GR-15310 Athens, Greece (e-mail: nsagias@ieee.org).

Digital Object Identifier 10.1109/TVT.2006.883803

0018-9545/$25.00 © 2007 IEEE

the derivation of a solution in the form of bounds. The use of bounds, as opposed to the aforementioned analytical solutions, can serve as a safe method of tackling the performance of EGC receivers in a computational efficient and easy way.

In this paper, the benefits of employing predetection EGC receivers in cellular radio networks are being addressed and studied in terms of tabulated functions. In this effort, independent but not necessarily identically distributed Nakagami-m fading and multiple Rayleigh distributed cochannel interferers are being considered. The presented analysis is not only limited to equal average fading power interferers, but the important case of distinct average powers, which more accurately describes realistic cellular wireless channels, is also examined. By following the coherent interference power calculation, novel closed-form expressions for the moments of the EGC output SINR are derived, which are used to study the average output SINR. Additionally, by assuming an interference-limited fading scenario and using a probability density function (pdf) of a lower bound (LB) of the sum of Nakagami-m fading envelopes, novel upper bounds (UBs) for the outage probability (OP) and the average symbol error probability (ASEP) for several constant envelope modulation schemes as well as LBs for the Shannon average spectral efficiency (ASE) are obtained in closed form. Computer-simulation results are also presented in order to verify the tightness of the proposed union bounds.

The remainder of this paper is organized as follows. Section II presents the system and channel model, while in Section III, closed-form expressions for the moments of the EGC output SINR are derived. In Section IV, union bounds for the OP, ASEP, and ASE are obtained in closed form. Numerical and computer simulations results are presented and compared in Section V, while concluding remarks are given in Section VI.

II. System and Channel Model

Let us consider an N-branch predetection EGC receiver where the desired component of the received signal in each branch undergoes frequency flat fading and AWGN, while it is being corrupted by L independent Rayleigh cochannel interferers. Matched filters with root raised-cosine (RRC) frequency response are being employed at both the transmitter and at the receiver sides. In each branch, the signal is passed through the RRC filter and the sampler, while perfect timing synchronization for the desired user is assumed. After cophasing the received signals in each branch with respect to the phase $\Phi_\ell (\ell = 1, 2, \ldots, N)$ of the corresponding desired component and then summed, the complex baseband signal at the output of the EGC receiver can be expressed as

$$S = d_0 \sum_{i=1}^{N} R_i + \sum_{k=1}^{L} \sum_{j=1}^{N} d_k \underbrace{X_{k,j} \exp\left[\jmath(\Theta_{k,j} - \Phi_j)\right]}_{G_{k,j}} + \sum_{i=1}^{N} C_i \exp(-\jmath\Phi_i) \quad (1)$$

where d_0 and d_ν $(\nu = 1, 2, \ldots, L)$ are the desired and νth interfering complex transmitted symbols, respectively, with average energy[1] $E_s = \mathcal{E}\langle |d_0|^2 \rangle = \mathcal{E}\langle |d_\nu|^2 \rangle$ ($\mathcal{E}\langle\cdot\rangle$ denotes expectation), C_ℓ is the AWGN complex sample in the ℓth input branch having single-sided power spectral density N_0 identical to all branches, and $\jmath = \sqrt{-1}$. By R_ℓ, the instantaneous fading envelope of the desired component of the received signal in the ℓth input branch is denoted, with its pdf to be given by

$$f_{R_\ell}(x) = \left(\frac{m_\ell}{\Omega_\ell}\right)^{m_\ell} \frac{x^{2m_\ell - 1}}{\Gamma(m_\ell)} \exp\left(-\frac{m_\ell}{\Omega_\ell} x^2\right) \quad (2)$$

where $\Omega_\ell = \mathcal{E}\langle R_\ell^2 \rangle$ and $m_\ell \geq 1/2$ are the average fading power and the Nakagami-m fading parameter, respectively, and $\Gamma(\cdot)$ is the Gamma function [23, eq. (8.310/1)]. Moreover, in (1), $G_{\nu,\ell} = X_{\nu,\ell} \exp[\jmath\,(\Theta_{\nu,\ell} - \Phi_\ell)]$ is a zero-mean Gaussian complex random variable (RV), expressing the channel gain of the νth interferer in the ℓth input branch multiplied by the cophasing factor $\exp(-\jmath\Phi_\ell)$, with $(\Theta_{\nu,\ell} - \Phi_\ell)$ being uniformly distributed in $[0, 2\pi)$ and $X_{\nu,\ell}$ being Rayleigh distributed. We further consider equal average interferer's fading power to each receiver branch, i.e., $\mathcal{E}\langle X_{\nu,\ell}^2 \rangle = \overline{P}_\nu, \forall \ell$. The usual assumptions are also made that the desired and interfering components are uncorrelated with each other and that the channel is slow fading for both of them.

Similar to [19] and [20], by following the coherent interference power calculation and the Gaussian interference model [24], the instantaneous EGC output SINR per symbol can be expressed as

$$Z = \frac{E_s \left(\sum_{i=1}^{N} R_i\right)^2}{NN_0 + aE_s \sum_{i=1}^{L} \left|\sum_{k=1}^{N} G_{i,k}\right|^2} = \frac{\frac{E_s}{N_0}\left(\sum_{i=1}^{N} R_i\right)^2}{N + a\frac{E_s}{N_0}\sum_{i=1}^{L} I_i} \quad (3)$$

where $a = 1 - \rho/4$, with $0 \leq \rho \leq 1$ being the roll-off factor of both the transmitting and receiving RRC filters, and $I_\nu = |\sum_{k=1}^{N} G_{\nu,k}|^2$ is an exponentially distributed RV with pdf given by

$$f_{I_\nu}(x) = \frac{1}{\overline{I}_\nu} \exp\left(-\frac{x}{\overline{I}_\nu}\right) \quad (4)$$

where $\overline{I}_\nu = N\overline{P}_\nu$ is its corresponding average value. The sum of L exponentially distributed RVs, appearing in the denominator of (3), can be represented by another RV for the following two cases. In the case of equal interferers' powers, i.e., $\overline{P}_\nu = \overline{P}\ \forall \nu$, the pdf of $U = a\sum_{i=1}^{L} I_i$ is given by the Erlang distribution

$$f_U(x) = \frac{1}{(L-1)!(aN\overline{P})^L} x^{L-1} \exp\left(-\frac{x}{aN\overline{P}}\right) \quad (5a)$$

[1] Only constant envelope modulation schemes are being considered to be used with EGC.

with corresponding average power $\overline{U} = a\ L\ N\overline{P}$, while in the case of distinct interferers' powers, i.e., $\overline{P}_i \neq \overline{P}_j\ \forall i \neq j$, it is given by

$$f_U(x) = \frac{1}{aN} \sum_{k=1}^{L} \frac{\Pi_k}{\overline{P}_k} \exp\left(-\frac{x}{aN\overline{P}_k}\right) \tag{5b}$$

with corresponding average power $\overline{U} = a\ N \sum_{i=1}^{L} \overline{P}_i$, and

$$\Pi_\nu = \prod_{\substack{i=1 \\ i\neq\nu}}^{L} \frac{\overline{P}_\nu}{\overline{P}_\nu - \overline{P}_i}.$$

III. Statistics of the EGC Output SINR

In this section, novel closed-form expressions for the moments of the EGC output SINR are derived. The EGC average output SINR, which is considered as one of the best understood performance measures, is also studied based on the derived expressions for the moments.

Using (3), the nth-order moment of the EGC output SINR per symbol $\mu_n = \mathcal{E}\langle Z^n\rangle$ can be expressed as

$$\mu_n = \mathcal{E}\left\langle \left[\frac{1}{N+Y}\left(\sum_{i=1}^{N}\sqrt{\gamma_i}\right)^2\right]^n \right\rangle \tag{6}$$

where $\gamma_\ell = R_\ell^2 E_s/N_0$ is the instantaneous signal-to-noise ratio (SNR) per symbol of the desired component received in the ℓth input branch, and $Y = U\ E_s/N_0$. Since the desired and the interfering components are mutually independent, (6) can be written as

$$\mu_n = \mathcal{E}\left\langle \left(\sum_{i=1}^{N}\sqrt{\gamma_i}\right)^{2n}\right\rangle \mathcal{E}\left\langle \frac{1}{(N+Y)^n}\right\rangle. \tag{7}$$

The two mean terms appearing in the above equation can be evaluated separately. The first one can be derived by expanding $(\sum_{i=1}^{N}\sqrt{\gamma_i})^{2n}$ using the multinomial identity [25, eq. (24.1/2)], yielding

$$\mathcal{E}\left\langle \left(\sum_{i=1}^{N}\sqrt{\gamma_i}\right)^{2n}\right\rangle = (2n)! \sum_{k_1=0}^{2n}\sum_{k_2=0}^{2n}\cdots\sum_{k_N=0}^{2n} \mathcal{E}\left\langle \prod_{j=1}^{N}\frac{\gamma_j^{k_j/2}}{k_j!}\right\rangle \delta\left(\sum_{i=1}^{N} k_i, 2n\right) \tag{8}$$

where $\delta(i,j)$ is the Kronecker Delta function defined as $\delta(i,j) = 1$, when $i = j$, and zero otherwise.[2] Moreover, since the desired components of the received signals are mutually independent with each other and by using the expression for nth-order moment of γ_ℓ [3, eq. (2.23)]

$$\mathcal{E}\langle \gamma_\ell^n\rangle = \frac{\Gamma(m_\ell + n)}{\Gamma(m_\ell) m_\ell^n}\overline{\gamma}_\ell^n \tag{9}$$

the term $\mathcal{E}\langle\prod_{j=1}^{N}\gamma_j^{k_j/2}\rangle$ in (8) can be expressed as

$$\mathcal{E}\left\langle \prod_{j=1}^{N}\gamma_j^{k_j/2}\right\rangle = \prod_{j=1}^{N}\frac{\Gamma(m_j + k_j/2)}{\Gamma(m_j) m_j^{k_j/2}}\overline{\gamma}_j^{k_j/2} \tag{10}$$

where $\overline{\gamma}_\ell = \Omega_\ell E_s/N_0$ is the average SNR per symbol of the desired component of the received signal in the ℓth input branch. Depending on whether the average fading powers of the interferers are equal or distinct, two cases are being studied next.

A. Equal Average Interferers' Powers

The second mean term in (7) can be obtained by averaging $1/(N+Y)^n$ over the pdf of Y, i.e.,

$$\mathcal{E}\left\langle \frac{1}{(N+Y)^n}\right\rangle = \int_0^\infty \frac{1}{(N+x)^n} f_Y(x)\, dx \tag{11}$$

in which using (5a) and [23, eq. (3.383/5)] leads to

$$\mathcal{E}\left\langle \frac{1}{(N+Y)^n}\right\rangle = \frac{N^{-n}}{(a\overline{P})^L}\Psi\left(L, L+1-n; \frac{1}{a\overline{P}}\right) \tag{12}$$

where $\Psi(x,y;z)$ $(x,y,z \in \Re)$ is the confluent hypergeometric function defined in [23, eq. (9.210/2)] as

$$\Psi(x,y;z) \stackrel{\triangle}{=} \frac{\Gamma(1-y)}{\Gamma(x+1-y)}{}_1F_1(x,y;z) + \frac{\Gamma(y-1)}{\Gamma(x)} z^{1-y}{}_1F_1(x+1-y, 2-y; z)$$

where ${}_1F_1(\cdot,\cdot;\cdot)$ is the Kummer confluent hypergeometric function [23, eq. (9.210/1)]. By substituting (8), (10), and (12) in (7), the nth-order moment of the instantaneous EGC output SINR per symbol with equal average interferers' powers can be expressed in closed form as

$$\mu_n = \frac{(2n)! N^{-n}}{(a\overline{P})^L}\Psi\left(L, L+1-n; \frac{1}{a\overline{P}}\right) \times \sum_{\substack{k_1,k_2,\ldots,k_n=0 \\ k_1+k_2+\cdots+k_n=2n}}^{2n} \prod_{j=1}^{N}\frac{\Gamma(m_j+k_j/2)}{k_j!\Gamma(m_j) m_j^{k_j/2}}\overline{\gamma}_j^{k_j/2}. \tag{13}$$

1) EGC Average Output SINR: The average output SINR can be easily derived in closed form, since it requires only the first moment of the output SINR, yielding

$$\overline{Z} = \frac{2}{N}\exp\left(\frac{1}{a\overline{P}}\right)\frac{1}{(a\overline{P})^L}\Gamma\left(1-L, \frac{1}{a\overline{P}}\right) \times \sum_{\substack{k_1,k_2,\ldots,k_N=0 \\ k_1+k_2+\cdots+k_N=2}}^{2} \prod_{j=1}^{N}\frac{\Gamma(m_j+k_j/2)}{k_j!\Gamma(m_j) m_j^{k_j/2}}\overline{\gamma}_j^{k_j/2} \tag{14}$$

[2] From now on, in this paper, the complicated notation of multiple sums $\sum_{k_1=0}^{2n}\sum_{k_2=0}^{2n}\cdots\sum_{k_N=0}^{2n}\delta\left(\sum_{i=1}^{N}k_i, 2n\right)$ is alleviated and replaced by $\sum_{\substack{k_1,k_2,\ldots,k_N=0 \\ k_1+k_2+\cdots+k_N=2n}}^{2n}$ for presentation purposes.

where $\Gamma(\cdot,\cdot)$ is the upper incomplete Gamma function [23, eq. (8.350/2)].

B. Distinct Average Interferers' Powers

In the case of interferers having distinct average fading powers, similar to the previous section, the second mean term in (7) can be obtained by substituting (5b) in (11) and using [23, eq. (3.353/2)] as

$$\mathcal{E}\left\langle \frac{1}{(N+Y)^n} \right\rangle = \frac{1}{(n-1)!}\sum_{k=1}^{L}\frac{\Pi_k}{\overline{P}_k}\left(\frac{-1}{aN\overline{P}_k}\right)^{n-1} \times \left[\sum_{t=1}^{n-1}(t-1)!\left(\frac{-1}{a\overline{P}_k}\right)^{-t} - \exp\left(\frac{1}{a\overline{P}_k}\right)E_i\left(\frac{-1}{a\overline{P}_k}\right)\right] \quad (15)$$

where $E_i(\cdot)$ is the exponential integral function [23, eq. (8.211/1)]. By substituting (8), (10), and (15) in (7), the nth-order moment of the instantaneous EGC output SINR per symbol with distinct average interferers' powers can be expressed in closed form as

$$\mu_n = \frac{(2n)!}{(n-1)!}\sum_{k=1}^{L}\frac{\Pi_k}{\overline{P}_k}\left(\frac{-1}{aN\overline{P}_k}\right)^{n-1} \times \left[\sum_{t=1}^{n-1}(t-1)!\left(\frac{-1}{a\overline{P}_k}\right)^{-t} - \exp\left(\frac{1}{a\overline{P}_k}\right)E_i\left(\frac{-1}{a\overline{P}_k}\right)\right] \times \sum_{\substack{k_1,k_2,\ldots,k_N=0\\ k_1+k_2+\cdots+k_N=2n}}^{2n}\prod_{j=1}^{N}\frac{\Gamma(m_j+k_j/2)}{k_j!\Gamma(m_j)m_j^{k_j/2}}\overline{\gamma}_j^{k_j/2}. \quad (16)$$

1) EGC Average Output SINR: By setting $n=1$ in (16), the EGC average output SINR can be easily derived as

$$\overline{Z} = \frac{2}{aN}\sum_{k=1}^{L}\frac{\Pi_k}{\overline{P}_k}\exp\left(\frac{1}{a\overline{P}_k}\right)\Gamma\left(0,\frac{1}{a\overline{P}_k}\right) \times \sum_{\substack{k_1,k_2,\ldots,k_N=0\\ k_1+k_2+\cdots+k_N=2}}^{2}\prod_{j=1}^{N}\frac{\Gamma(m_j+k_j/2)}{k_j!\Gamma(m_j)m_j^{k_j/2}}\overline{\gamma}_j^{k_j/2}. \quad (17)$$

IV. Interference-Limited Environment

Let us consider the system and channel model presented in Section II, and further assume that CCI is the limiting source of performance degradation [26]. Hence, the thermal noise is ignored and an interference-limited environment is being considered. According to this scenario, from (3), the instantaneous signal-to-interference ratio (SIR) at the output of the EGC can be expressed as

$$\gamma = \frac{1}{U}\left(\sum_{i=1}^{N}R_i\right)^2. \quad (18)$$

By applying the well-known inequality between the arithmetic and geometric mean [23, Sec. 11.116] to RVs R_ℓ, i.e.,

$$\frac{1}{N}\sum_{i=1}^{N}R_i \geq \prod_{i=1}^{N}R_i^{1/N} \quad (19)$$

(18) can be lower bounded as

$$\gamma \geq \gamma^* = N^2\frac{\mathcal{P}^{2/N}}{U} \quad (20)$$

where the RV $\mathcal{P}$ is defined as the product of R_ℓ, i.e., $\mathcal{P} \triangleq \prod_{i=1}^{N}R_i$, with pdf given by [27, eq. (8)]

$$f_{\mathcal{P}(x)} = \frac{2x^{-1}}{\prod_{i=1}^{N}\Gamma(m_i)}G_{0,N}^{N,0}\left[x^2\prod_{i=1}^{N}\left(\frac{m_i}{\Omega_i}\right)\middle|\begin{matrix}-\\ m_1,m_2,\ldots,m_n\end{matrix}\right] \quad (21)$$

where $G[\cdot]$ is the Meijer's G-function[3] [23, eq. (9.301)]. It can be easily recognized that for the special case of $N=1$ and by using [28, eq. (11)], (21) reduces to (2). Moreover, for $N=2$ and by using [23, eq. (9.34/3)], (21) reduces to [29]

$$f_{\mathcal{P}}(x) = \frac{4y^{m_1+m_2-1}}{\prod_{i=1}^{2}\Gamma(m_i)(\Omega_i/m_i)^{(m_1+m_2)/2}} \times K_{m_1-m_2}\left(2y\prod_{i=1}^{2}\sqrt{\frac{m_i}{\Omega_i}}\right) \quad (22)$$

where $K_{m_1-m_2}(\cdot)$ is the (m_1-m_2)th-order modified Bessel function of the second kind [23, eq. (8.432/1)].

Since RVs $\mathcal{P}$ and U are mutually independent, by using (20) and [30, eq. (6.43)], the pdf of an LB of γ, i.e., the pdf of γ^*, can be derived as

$$f_{\gamma^*}(x) = \frac{N}{2N^N}\int_0^\infty y(xy)^{N/2}f_{\mathcal{P}}\left[\left(\frac{xy}{N^2}\right)^{N/2}\right]f_U(y)dy. \quad (23)$$

Next, the performances of EGC are studied for the two cases of equal and distinct average interferers' fading powers.

A. Equal Average Interferers' Powers

By substituting (5a) and (21) in (23), an integral of the form

$$\int_0^\infty y^{L-1}\exp\left(-\frac{y}{aN\overline{P}}\right) \times G_{0,N}^{N,0}\left[y^N\prod_{i=1}^{N}\left(\frac{m_i}{\Omega_i}\right)\middle|\begin{matrix}-\\ m_1,m_2,\ldots,m_n\end{matrix}\right]dy$$

[3]By applying the transformation given by [23, eq. (9.303)] in (21), $G[\cdot]$ can be expressed in terms of more widely used functions, such as the generalized hypergeometric [23, eq. (9.14), (1)]. Note that both the Meijer's G-function and generalized hypergeometric function are included as built-in functions in most of the popular mathematical software packages such as Maple and Mathematica.

arises, which is not included in tables of classical reference books such as [23]. By expressing the exponential functions as Meijer's G-functions [28, eq. (11)], using [28, eq. (21)], and after some mathematical manipulations, the pdf of γ^* can be derived as

$$f_{\gamma^*}(x) = \frac{N^{L+1/2}(\sqrt{2\pi})^{1-N}}{(L-1)!\prod_{i=1}^{N}\Gamma(m_i)}x^{-1} \times G_{N,N}^{N,N}\left[x^N\prod_{i=1}^{N}\left(\frac{am_i}{\mathcal{R}_i}\right)\middle|\begin{matrix}\Delta(N;1-L)\\ m_1,m_2,\ldots,m_n\end{matrix}\right] \quad (24)$$

where $\mathcal{R}_\ell = \Omega_\ell/\overline{P}$ is the average SIR in the ℓth input branch, and $\Delta(n;x)$ is defined as $\Delta(n;x) \triangleq x/n,(x+1)/n,\ldots,(x+n-1)/n$, with x an arbitrary real value and n a positive integer.

1) OP: The OP is defined as the probability that the instantaneous SIR falls below a given outage threshold $\gamma_{\rm th}$. Starting with

$$P_{\rm out}(\gamma_{\rm th}) \le \int_0^{\gamma_{\rm th}} f_{\gamma^*}(x)dx \quad (25)$$

substituting (24), and by using [28, eq. (26)], an UB for the OP can be obtained in a closed form as

$$P_{\rm out}(\gamma_{\rm th}) \le \frac{N^{L-1/2}(\sqrt{2\pi})^{1-N}}{(L-1)!\prod_{i=1}^{N}\Gamma(m_i)} \times G_{N+1,N+1}^{N,N+1}\left[\gamma_{\rm th}^N\prod_{i=1}^{N}\left(\frac{am_i}{\mathcal{R}_i}\right)\middle|\begin{matrix}\Delta(N;1-L),1\\ m_1,m_2,\ldots,m_n,0\end{matrix}\right]. \quad (26)$$

2) ASEP: A straightforward approach to obtain a UB for the ASEP $\overline{P}_{\rm se}$ is to average the conditional symbol error probability $P_{\rm se}(\gamma)$ over the pdf of γ^*, i.e.,

$$\overline{P}_{\rm se} \le \int_0^{\infty} P_{\rm se}(x)f_{\gamma^*}(x)dx. \quad (27)$$

Since the EGC does not require estimation of the fading amplitudes, it is often limited in practice only to coherent modulations with equal-energy symbols (e.g., M-PSK). However, in many applications either the phases of the received signals can be tracked accurately, and it is therefore not possible to perform a coherent detection. In such scenarios, communication systems must rely on noncoherent detection techniques (e.g., frequency shift keying, differential phase shift keying, etc) [3, Sec. 8]. For $P_{\rm se}(\gamma)$, there are two well-known generic expressions for the aforementioned sets of modulation schemes, including

1) binary frequency shift keying (BFSK) and for higher values of average SIR, M-PSK, M-ary-differentially encoded phase shift keying (M-DEPSK), with $M \ge 2$, and minimum shift keying (MSK), in the form of

$$P_{\rm se}(\gamma) = A\,\mathrm{erfc}(\sqrt{B\gamma}) \quad (28)$$

where $\mathrm{erfc}(\cdot)$ is the well-known complementary error function [23, eq. (8.250/4)];

2) noncoherent BFSK (NBFSK) and binary differential phase shift keying (BDPSK) in the form of

$$P_{\rm se}(\gamma) = A\,\exp(-B\gamma). \quad (29)$$

In the above expressions for $P_{\rm se}(\gamma)$, the particular values of A and B depend on the specific modulation scheme employed and can be found in [31]. Next, (27) is solved in closed form for each one of the above two sets of signals.

Using (24), (27), and (28), it can be easily recognized that for the first set of modulated schemes (i.e., BFSK, M-PSK, M-DEPSK, and MSK), the evaluation of definite integrals, which include Meijer's, power, and exponential functions, is required. Since these kinds of integrals are not tabulated, the solution can be found with the aid of [28, eq. (21)] so that the UB for the ASEP can be expressed in closed form as

$$\overline{P}_{\rm se} \le \frac{AN^{L-1/2}(2\pi)^{1-N}}{\sqrt{\pi}(L-1)!\prod_{i=1}^{N}\Gamma(m_i)} \times G_{3N,2N}^{N,3N}\left[\prod_{i=1}^{N}\left(\frac{aNm_i}{B\mathcal{R}_i}\right)\middle|\begin{matrix}\Delta(N;1-L),\Delta(N;1),\Delta(N;1/2)\\ m_1,m_2,\ldots,m_N,\Delta(N;0)\end{matrix}\right]. \quad (30)$$

Similarly, by substituting (24) and (29) in (27) and by using [28, eq. (21)], for the second set of modulation schemes (i.e., NBFSK and BDPSK), a UB for the ASEP can be derived as

$$\overline{P}_{\rm se} \le \frac{AN^{L}(2\pi)^{1-N}}{(L-1)!\prod_{i=1}^{N}\Gamma(m_i)} \times G_{2N,N}^{N,2N}\left[\prod_{i=1}^{N}\left(\frac{aNm_i}{B\mathcal{R}_i}\right)\middle|\begin{matrix}\Delta(N;1-L),\Delta(N;1)\\ m_1,m_2,\ldots,m_N\end{matrix}\right]. \quad (31)$$

3) ASE: The Shannon capacity of a channel defines its theoretical UB for the maximum data transmission rate at an arbitrarily small bit error rate without any delay or complexity constraints. Therefore, the Shannon capacity represents an optimistic bound for practical communication schemes and also serves as a benchmark against which to compare the spectral efficiency of all practical adaptive transmission schemes [32]. Let ξ be the SIR in an interference-limited environment without fading; then, the Shannon spectral efficiency is given by[4]

$$S_e(\xi) = \log_2(1+\xi). \quad (32)$$

As (32) reads, in a channel with fading where $\xi = \gamma$ is an RV, $S_e(\gamma)$ is also another RV. Hence, an LB for the ASE can be obtained by averaging $\log_2(1+\gamma)$ over the pdf of γ^* [32], [34]–[40], i.e.,

$$\overline{S}_e \ge \int_0^{\infty} \log_2(1+x)f_{\gamma^*}(x)dx. \quad (33)$$

[4]The Shannon's capacity formula given by (32) assumes Gaussian distributed noise/interference [33, p. 263]. Since the sum of the interfering components is clearly not Gaussian distributed [see (3) and (4)], the spectral efficiency given by (32) provides an optimistic case compared to the Gaussian channel case.

By transforming the logarithm to a Meijer's G-function [28, eq. (11)], averaging over the pdf of γ^* as represented by (24) and (33), and using [28, eq. (21)], an LB for the ASE yields, in closed form

$$\overline{S}_e \geq \frac{N^{L-1/2}(\sqrt{2\pi})^{3(1-N)}}{\ln(2)(L-1)!\prod_{i=1}^{N}\Gamma(m_i)} \times G_{3N,3N}^{3N,2N}\left[\prod_{i=1}^{N}\left(\frac{am_i}{\mathcal{R}_i}\right)\middle|\begin{matrix}\Delta(N;1-L),\Delta(N;0),\Delta(N;1)\\ m_1,m_2,\ldots,m_n,\Delta(N;0),\Delta(N;0)\end{matrix}\right]. \quad (34)$$

By using (26) and (32), the UB for the outage spectral efficiency can be also derived in a simple closed-form expression as

$$P_{\rm ase}(\gamma_{\rm th}) \leq P_{\rm out}(2^{\gamma_{\rm th}}-1). \quad (35)$$

B. Distinct Average Interferers' Powers

By substituting (5b) and (21) in (23) and by using [28, eq. (21)], the pdf of γ^* can be derived as

$$f_{\gamma^*}(x) = \frac{N^{3/2}(\sqrt{2\pi})^{1-N}}{\prod_{i=1}^{N}\Gamma(m_i)}x^{-1} \times \sum_{k=1}^{L}\Pi_k G_{N,N}^{N,N}\left[x^N\prod_{i=1}^{N}\left(\frac{am_i}{\mathcal{R}_i}\right)\middle|\begin{matrix}\Delta(N;0)\\ m_1,m_2,\ldots,m_n\end{matrix}\right] \quad (36)$$

where $\mathcal{R}_{\ell,\nu} = \Omega_\ell/\overline{P}_\nu$ is the average SIR in the ℓth input branch from the νth interferer.

1) OP: Starting with (25), substituting (36), and by using [28, eq. (26)], the UB for the OP can be obtained in closed form as

$$P_{\rm out}(\gamma_{\rm th}) \leq \frac{\sqrt{N}(\sqrt{2\pi})^{1-N}}{\prod_{i=1}^{N}\Gamma(m_i)}\sum_{k=1}^{L}\Pi_k \times G_{N+1,N+1}^{N,N+1}\left[\gamma_{\rm th}^N\prod_{i=1}^{N}\left(\frac{am_i}{\mathcal{R}_i,k}\right)\middle|\begin{matrix}\Delta(N;0),1\\ m_1,m_2,\ldots,m_N,0\end{matrix}\right]. \quad (37)$$

2) ASEP: By substituting (28) and (36) in (27) and by using [28, eq. (21)], for BFSK, M-PSK, M-DEPSK, and MSK, the UB for the ASEP can be expressed in closed form as

$$\overline{P}_{\rm se} \leq \frac{A\sqrt{N}(2\pi)^{1-N}}{\sqrt{\pi}\prod_{i=1}^{N}\Gamma(m_i)}\sum_{k=1}^{L}\Pi_k \times G_{3N,2N}^{N,3N}\left[\prod_{i=1}^{N}\left(\frac{aNm_i}{B\mathcal{R}_{i,k}}\right)\middle|\begin{matrix}\Delta(N;0),\Delta(N;1),\Delta(N;1/2)\\ m_1,m_2,\ldots,m_N,\Delta(N;0)\end{matrix}\right]. \quad (38)$$

Similarly, by using (29), for NBFSK and BDPSK, the UB for the ASEP can be also derived as

$$\overline{P}_{\rm se} \leq \frac{AN(2\pi)^{1-N}}{\prod_{i=1}^{N}\Gamma(m_i)} \times \sum_{k=1}^{L}\Pi_k G_{2N,N}^{N,2N}\left[\prod_{i=1}^{N}\left(\frac{aNm_i}{B\mathcal{R}_{i,k}}\right)\middle|\begin{matrix}\Delta(N;0),\Delta(N;1)\\ m_1,m_2,\ldots,m_N\end{matrix}\right]. \quad (39)$$

3) ASE: By substituting (36) in (33) and following a similar procedure for the derivation of (34), an LB for the ASE in case of interferers having distinct average fading powers can be obtained in closed form as

$$\overline{S}_e \geq \frac{\sqrt{N}(\sqrt{2\pi})^{3(1-N)}}{\ln(2)\prod_{i=1}^{N}\Gamma(m_i)}\sum_{k=1}^{L}\Pi_k \times G_{3N,3N}^{3N,2N}\left[\prod_{i=1}^{N}\left(\frac{am_i}{\mathcal{R}_{i,k}}\right)\middle|\begin{matrix}\Delta(N;0),\Delta(N;0),\Delta(N;1)\\ m_1,m_2,\ldots,m_n,\Delta(N;0),\Delta(N;0)\end{matrix}\right]. \quad (40)$$

Using (35) and (37), the UB for the outage ASE can be also derived in a simple closed form.

V. Numerical and Computer Simulation Results

In this section, representative performance evaluation results for N-branch EGC receivers operating in the presence of multipath fading and CCI, such as the normalized average output SINR, OP, ABEP, and ASE, are presented. Without loss of generality, the results are for identical values $(m_\ell = m)$ and integer-order fading parameters. The use of integer order for m facilitates comparisons between the numerical and computer simulation[5] results. When nonidentical desired components and/or interferers having distinct average powers are being considered, exponentially power delay profiles (PDPs), which are determined by

$$\Omega_\ell = \Omega_1\exp\left[-\delta_D(\ell-1)\right] \quad (41a)$$

and/or

$$\overline{P}_\nu = \overline{P}_1\exp\left[-\delta_i(\nu-1)\right] \quad (41b)$$

are being assumed, respectively, with δ_D and δ_I being the respective power decaying factors.

By numerically evaluating (14) and (17), curves for the EGC average output SINR normalized by the average SNR of the first input branch $\overline{Z}/\overline{\gamma}_1$ are demonstrated in Figs. 1 and 2, respectively, for a roll-off factor $\rho = 0.8$. For the case of identical desired components and equal average power interferers, in Fig. 1, $\overline{Z}/\overline{\gamma}_1$ is plotted as a function of the number of diversity input branches N for several values of the number of interferers L and various m. It can be easily recognized that as N and/or m increases, $\overline{Z}/\overline{\gamma}_1$ also increases. Moreover, as L increases,

[5]As it is known, the use of integer-order values of m significantly simplifies the procedure for the generation of Nakagami-m RVs.

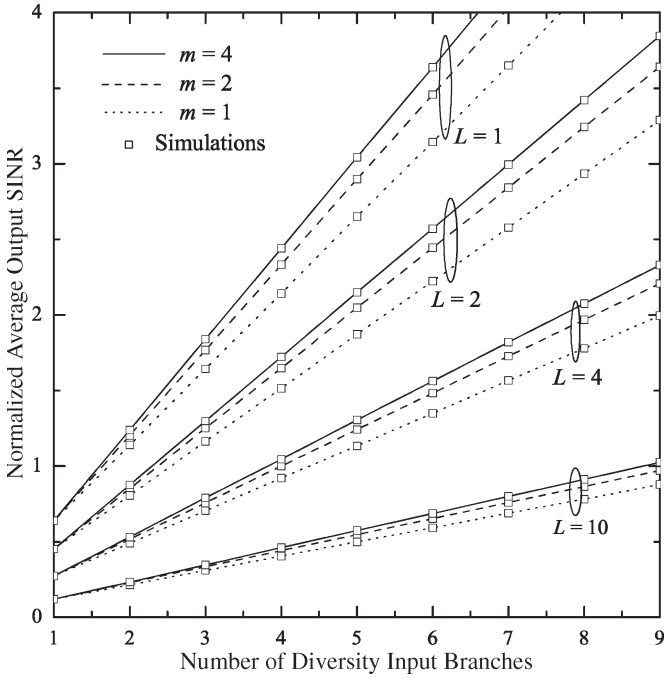

Fig. 1. EGC normalized average output SINR as a function of the number of diversity input branches for equal average fading powers for both the desired component and interferers.

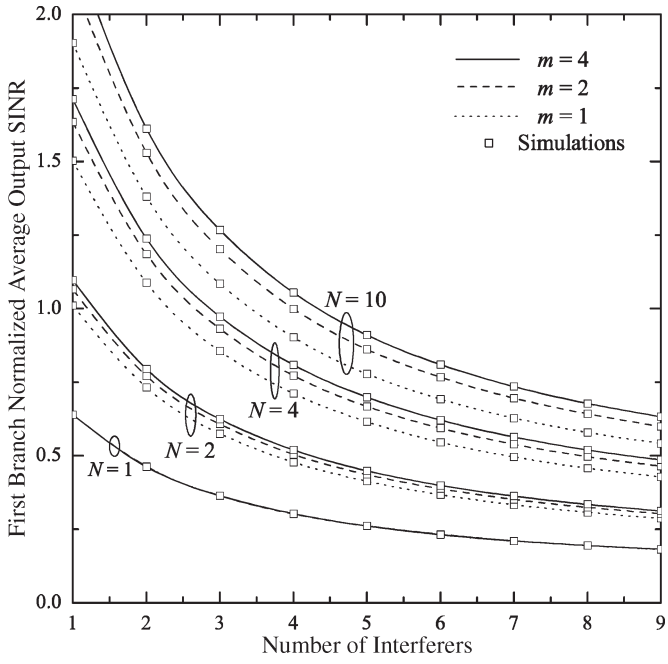

Fig. 2. EGC first branch normalized average output SINR as a function of the number of interferers for both distinct desired component and interferers.

$\overline{Z}/\overline{\gamma}_1$ decreases, while m seems to have minor effect on $\overline{Z}/\overline{\gamma}_1$ compared to L. Similar behavior is also observed in Fig. 2, in which $\overline{Z}/\overline{\gamma}_1$ is plotted as a function of L for several values of N with nonidentical desired components and interferers having distinct average powers, with $\delta_D = 0.25$ and $\delta_I = 0.1$, respectively, and for the same values of m as in Fig. 1. Computer simulation results (marked with squares) are also included in both figures, and a perfect match between these different sets of results can be observed, verifying the presented mathematical analysis. From Figs. 1 and 2, an interesting finding is that, especially for small values of L, $\overline{Z}/\overline{\gamma}_1$ rapidly decreases as L increases. For example, from Fig. 2, for $N = 4$ and $m = 4$, the degradation from $L = 1$ to $L = 4$ is 53%, while from $L = 4$ to $L = 7$, it is only 15%. Based on this observation, it may be concluded that the performance of cellular radio networks in the uplink is degraded mainly by the first tier of interferers (adjacent cells).

Having numerically evaluated (26) and (27), performance UBs for the OP P_{out} for a three-branch $(N = 3)$ EGC receiver are presented in Figs. 3 and 4, respectively, as a function of the normalized to $\mathcal{R}_1$ outage threshold $\gamma_{\text{th}}/\mathcal{R}_1$ with an exponentially decaying PDP for the desired components of the received signals with $\delta_D = 0.2$ and for several values of m and L. Fig. 3 is plotted for equal average interferers' powers, while in Fig. 4, distinct average interferers' powers with $\delta_I = 0.2$ are being considered. As expected, the results clearly show that P_{out} improves with a decrease of L and/or $\gamma_{\text{th}}/\mathcal{R}_{1,1}$ and/or an increase of m. For comparison purposes, the curves for the corresponding exact P_{out}, obtained via computer simulations, are also included in these figures. By comparing the numerically evaluated results with the computer simulated ones, we deduce a close match between them. Specifically, as m increases, the

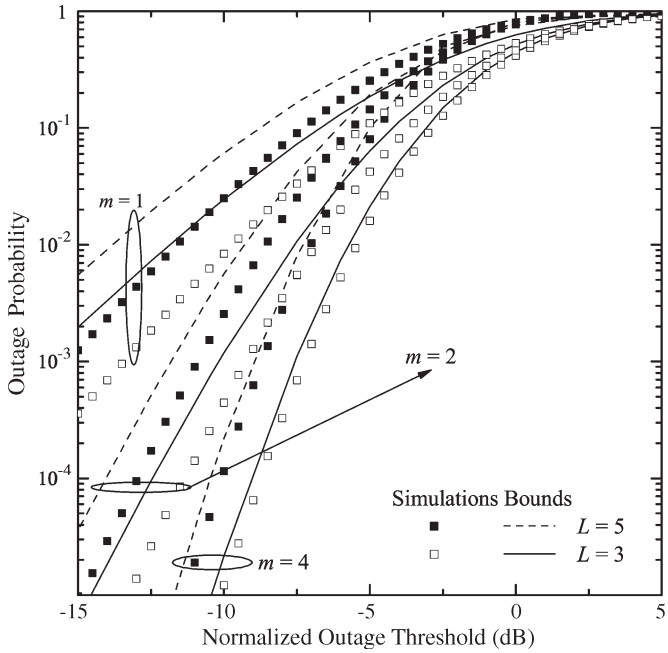

Fig. 3. OP as a function of the normalized outage threshold at the output of EGC receiver with three branches.

bounds become tighter. For example, from Fig. 4 for $L = 1$, and $P_{\text{out}} = 6 \times 10^{-4}$, for $m = 1$ and $m = 4$, the differences between exacts and bounds are 3 dB and less than 0.3 dB, respectively. The trend of the results can be explained as follows. As it is clear, the lower the difference between the terms of the left and right sides of (19), the tighter the bounds will be. In fact, equality in (19) holds if and only if all R_ℓ are equal to each other, i.e., $R_\ell = R \forall \ell$. For relatively large values of m, all fading envelopes R_ℓ will be with high probability close to their average value, and thus, it is expected that R_ℓ will take similar values.

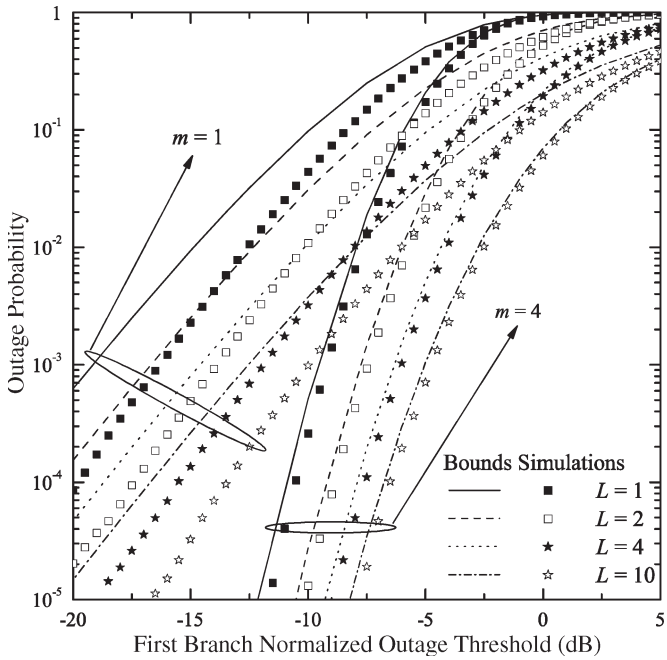

Fig. 4. OP as a function of the normalized outage threshold for distinct average fading powers for both desired and interfering components at the output of EGC receiver with three branches.

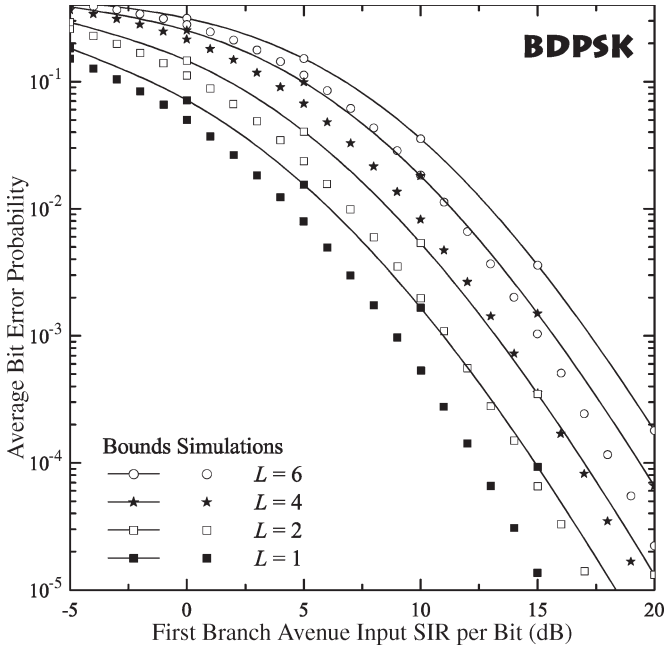

Fig. 5. ABEP performance of BDPSK signaling for an EGC receiver with four branches operating in a Rayleigh fading environment with nonidentically distributed desired components and equal average interferers' powers.

TABLE I
RELATIVE ERROR BETWEEN EXACTS AND BOUNDS FOR THE ABEP OF GRAY-ENCODED QPSK MODULATION SIGNALING FOR $\overline{\gamma}_b = 15$ dB

	Relative error, e_r ($L = 1$)			Relative error, e_r ($L = 6$)		
m	$N = 2$	$N = 3$	$N = 4$	$N = 2$	$N = 3$	$N = 4$
1	24.19%	43.49%	60.53%	8.64%	15.99%	22.80%
2	11.74%	19.96%	26.76%	4.48%	8.11%	11.37%
3	7.60%	12.70%	16.73%	2.98%	5.37%	7.50%
4	5.58%	9.25%	12.16%	2.24%	4.01%	5.56%
5	4.39%	7.27%	9.52%	1.79%	3.19%	4.44%

Using (30) and (31) for equal and (38) and (39) for distinct average power interferers, ASEP performance UBs for an N-branch EGC receiver, operating in the presence of Nakagami-m fading and CCI, can be numerically evaluated for various constant envelope coherent or noncoherent and binary or multilevel modulation schemes. In Table I, relative error values

$$e_{\mathrm{r}} = \frac{\overline{P}_{\mathrm{be}} - \widetilde{P}_{\mathrm{be}}}{\widetilde{P}_{\mathrm{be}}} \times 100\% \tag{42}$$

between exacts (computer simulations), $\widetilde{P}_{\mathrm{be}}$, and bounds $\overline{P}_{\mathrm{be}} = \overline{P}_{\mathrm{se}}/\log_2(M)$ for the ABEP performance are summarized. The presented results have been obtained for a fixed value of the average SIR per bit $\overline{\gamma}_b = \mathcal{R}_1/\log_2(M) = 15$ dB, Gray-encoded quadrature phase shift keying (QPSK) ($M = 4$) modulation signaling, equal average fading powers both desired components and interferers, $\rho = 1$, and several values of N, L, and m having practical interest. From Table I, it can be verified that e_{r} decreases as m and/or L increases, which is in agreement with corresponding findings for P_{out}. Moreover, the lower the value of N, the tighter the bounds will be. This occurs because both bounds and exact results move toward a fixed UB, which is obtained for $N = 1$. Note that from (19), it

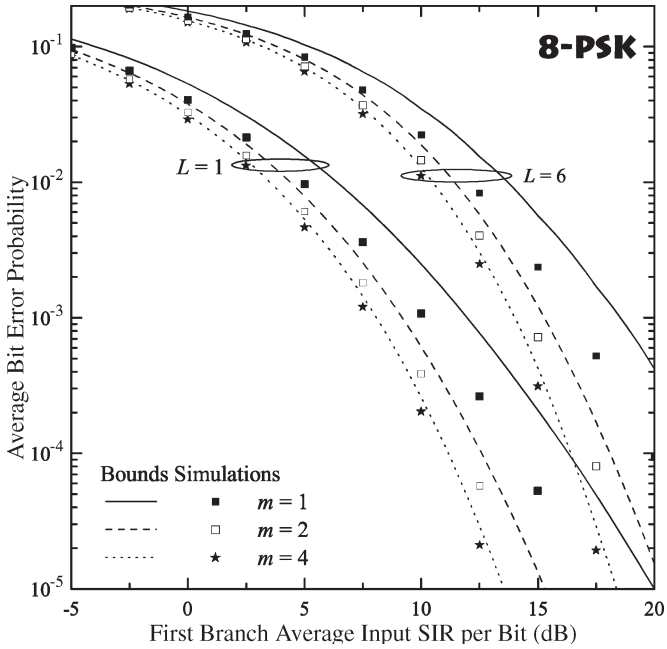

Fig. 6. ABEP performance of 8-PSK signaling for an EGC receiver with four branches operating in a Nakagami-m fading environment with nonidentically distributed average fading powers.

can be seen that for $N = 1$, $e_{\mathrm{r}} = 0$. From Table I, it becomes evident that for moderate values of N, e_{r} is less than a half order of magnitude, meaning that the proposed bounds are tight. Three indicative examples for the ABEP performances of BDPSK ($M = 2$), Gray-encoded 8-PSK ($M = 8$), and Gray-encoded M-PSK are illustrated in Figs. 5–7, respectively. In Fig. 5, $\overline{P}_{\mathrm{be}}$ is plotted as a function of the average SIR per bit of the first input branch $\overline{\gamma}_b = \mathcal{R}_{1,1}/\log_2(M)$ for nonidentically distributed desired components with a power decaying factor $\delta_D = 0.2$, $m = 1$, $N = 4$, $\rho = 1$, and for several values of L.

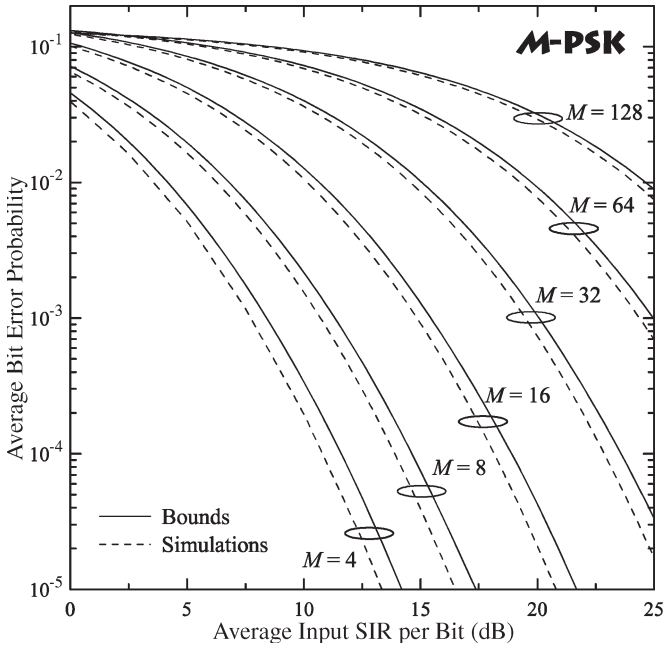

Fig. 7. ABEP performance of M-PSK signaling for an EGC receiver with three branches operating in an identical Nakagami-m fading environment with $m = 2$, $L = 2$, and interferers with distinct average powers.

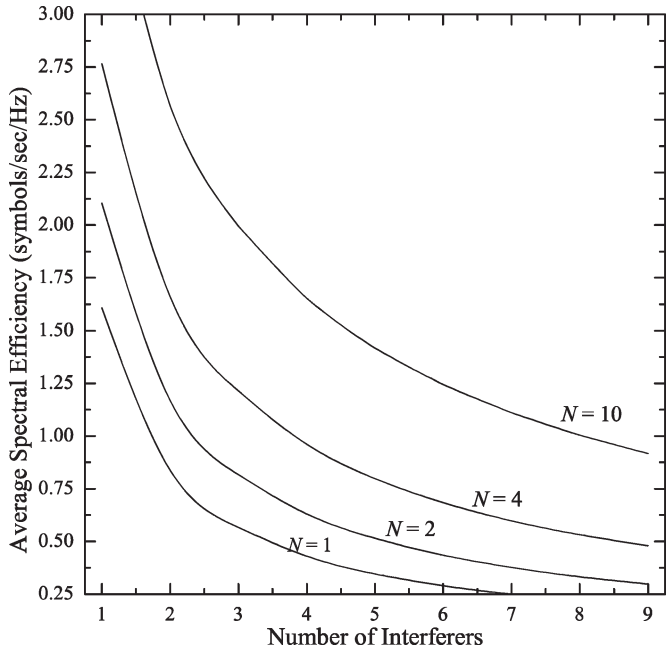

Fig. 8. LBs for the ASE performance of an EGC receiver operating over a Rayleigh environment with equal average fading powers for both desired components and interferers.

As expected, the obtained performance evaluation results show that $\overline{P}_{\rm be}$ improves with an increase of N and/or m. In Fig. 6, $\overline{P}_{\rm be}$ is plotted as a function of $\overline{\gamma}_b$ for 8-PSK signaling, $N = 4$, $\rho = 0.8$, and for several values of L and m. Furthermore, in Fig. 7, $\overline{P}_{\rm be}$ of M-PSK is plotted as a function of $\overline{\gamma}_b$ for $\delta_I = 0.2$, $\rho = 0.75$, $N = 3$, $L = 2$, $m = 2$, and for several values of the modulation order M. It is clear that as M increases, $\overline{P}_{\rm be}$ degrades. For comparison purposes, exact results obtained by means of computer simulations are also included in Figs. 5–7, verifying the tightness of the proposed bounds. As in Figs. 3 and 4, the numerically evaluated results for the bounded ABEPs are close to the simulated ones, while as previously mentioned, the higher m, the tighter the bounds will be.

Using (34) and (40), Figs. 8 and 9 demonstrate LBs for ASE, called $\overline{S}_e$, for both equal and distinct desired ($\delta_D = 0.2$) and interfering components ($\delta_I = 0.1$) with $\rho = 0.8$. In Fig. 8, $\overline{S}_e$ is plotted as a function of L for a Rayleigh fading environment and for various N. As expected, $\overline{S}_e$ degrades with an increase of L and/or a decrease of N. Similar findings can be also extracted from Fig. 9, in which $\overline{S}_e$ is plotted as a function of $\mathcal{R}_{1,1}$ for $L = 6$. An interesting finding from both figures is that m has a minor effect on $\overline{S}_e$, compared the effect of L.

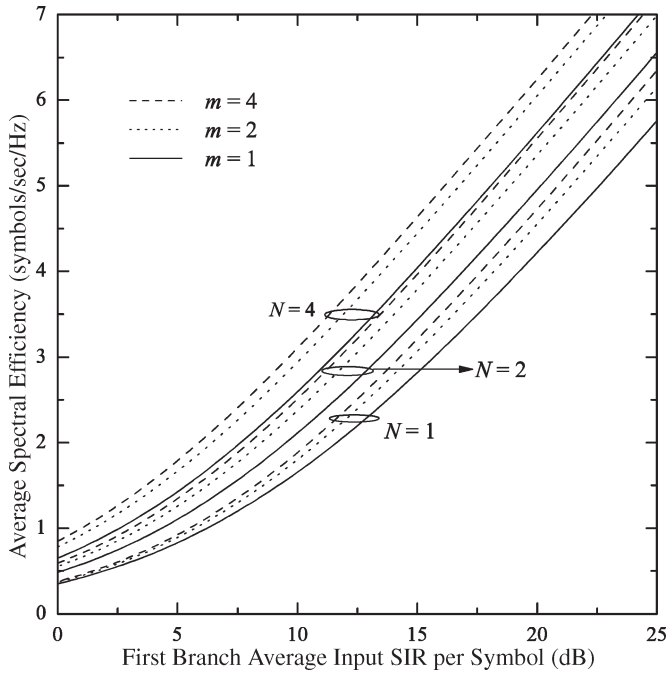

Fig. 9. LBs for the ASE performance of an EGC receiver operating over an environment with distinct average fading powers for both desired components and interferers.

VI. Conclusion

The performance of EGC receivers in the presence of multipath fading, multiple cochannel interferers, and AWGN was studied. By considering not-necessarily identical Nakagami-m desired and Rayleigh interfering components, novel closed-form expressions for the moments of the EGC output SINR were presented, and the corresponding average output SINR was extracted. Moreover, by assuming an interference-limited fading scenario and by using a distribution of an LB for the sum of Nakagami-m fading envelopes, novel union UBs for the OP and ASEP and LBs for the ASE were derived in closed form. Computer simulations were also performed to verify the tightness and the correctness of the proposed mathematical formulation, and it was concluded that the higher the value of Nakagami-m fading parameter and/or the number of interferers, the tighter the proposed bounds are. The results also show that the performance of cellular radio networks in the uplink is degraded mainly from the CCI of the adjacent cells of the first tier.

ACKNOWLEDGMENT

The author would like to thank Dr. G. K. Karagiannidis and the anonymous reviewers for their constructive suggestions, based on which, the quality of this paper has been considerably improved.

REFERENCES

[1] T. S. Rappaport, *Wireless Communications*. Englewood Cliffs, NJ: Prentice-Hall, 1996.

[2] W. C. Jakes, *Microwave Mobile Communications*. New York: Wiley, 1974.

[3] M. K. Simon and M.-S. Alouini, *Digital Communication Over Fading Channels*, 2nd ed. New York: Wiley, Jan. 2005.

[4] M.-S. Alouini and M. K. Simon, "Performance analysis of coherent equal gain combining over Nakagami-m fading channels," *IEEE Trans. Veh. Technol.*, vol. 50, no. 6, pp. 1449–1463, Nov. 2001.

[5] R. K. Mallik, M. Z. Win, and J. H. Winters, "Performance of dual diversity predetection EGC in correlated Rayleigh fading with unequal branch SNRs," *IEEE Trans. Commun.*, vol. 50, no. 7, pp. 1041–1044, Jul. 2002.

[6] G. K. Karagiannidis, D. A. Zogas, and S. A. Kotsopoulos, "BER performance of dual predetection EGC in correlative Nakagami-m fading," *IEEE Trans. Commun.*, vol. 52, no. 1, pp. 50–53, Jan. 2004.

[7] ——, "Statistical properties of the EGC output SNR over correlated Nakagami-m fading channels," *IEEE Trans. Wireless Commun.*, vol. 3, no. 5, pp. 1764–1769, Sep. 2004.

[8] G. K. Karagiannidis, "Moments-based approach to the performance analysis of equal gain diversity in Nakagami-m fading," *IEEE Trans. Commun.*, vol. 52, no. 5, pp. 685–690, May 2004.

[9] A. Annamalai, C. Tellambura, and V. K. Bhargava, "Exact evaluation of maximal-ratio and equal-gain diversity receivers for M-ary QAM on Nakagami-fading channels," *IEEE Trans. Commun.*, vol. 47, no. 9, pp. 1335–1344, Sep. 1999.

[10] N. C. Beaulieu and A. A. Abu-Dayya, "Analysis of equal gain diversity on Nakagami fading channels," *IEEE Trans. Commun.*, vol. 39, no. 2, pp. 225–234, Feb. 1991.

[11] Q. T. Zhang, "Probability of error for equal-gain combiners over Rayleigh channels: Some closed-form solutions," *IEEE Trans. Commun.*, vol. 45, no. 3, pp. 270–273, Mar. 1997.

[12] ——, "A simple approach to probability of error for equal gain combiners over Rayleigh channels," *IEEE Trans. Veh. Technol.*, vol. 48, no. 4, pp. 1151–1154, Jul. 1999.

[13] P. R. Sahu and A. K. Chaturvedi, "Performance analysis of predetection EGC receiver in Weibull fading channel," *Electron. Lett.*, vol. 41, no. 2, pp. 47–48, Jan. 2005.

[14] C.-D. Iskander and P. T. Mathiopoulos, "Performance of M-QAM with coherent equal-gain combining in correlated Nakagami-m fading," *Electron. Lett.*, vol. 39, no. 1, pp. 141–142, Jan. 2003.

[15] ——, "Performance of dual-branch coherent equal-gain combining in correlated Nakagami-m fading," *Electron. Lett.*, vol. 39, no. 15, pp. 1152–1154, Jul. 2003.

[16] ——, "Analytical level-crossing rates and average fade durations for diversity techniques in Nakagami fading channels," *IEEE Trans. Commun.*, vol. 50, no. 8, pp. 1301–1309, Aug. 2002.

[17] A. A. Abu-Dayya and N. C. Beaulieu, "Outage probabilities of diversity cellular systems with cochannel interference in Nakagami fading," *IEEE Trans. Veh. Technol.*, vol. 41, no. 4, pp. 343–355, Nov. 1992.

[18] ——, "Diversity MPSK receivers in cochannel interference," *IEEE Trans. Veh. Technol.*, vol. 48, no. 6, pp. 1959–1965, Nov. 1999.

[19] Y. Song, S. D. Blostein, and J. Cheng, "Exact outage probability for equal gain combining with cochannel interference in Rayleigh fading," *IEEE Trans. Wireless Commun.*, vol. 2, no. 5, pp. 865–870, Sep. 2003.

[20] ——, "Outage probability comparisons for diversity systems with cochannel interference in Rayleigh fading," *IEEE Trans. Wireless Commun.*, vol. 4, no. 4, pp. 1279–1284, Jul. 2005.

[21] K. Sivanesan and N. C. Beaulieu, "Exact BER analysis of bandlimited BPSK with EGC and SC diversity in cochannel interference and Nakagami fading," *IEEE Commun. Lett.*, vol. 8, no. 10, pp. 623–625, Oct. 2004.

[22] N. C. Sagias, G. K. Karagiannidis, D. A. Zogas, G. S. Tombras, and S. A. Kotsopoulos, "Average output SINR of equal-gain diversity in correlated Nakagami-m fading with cochannel interference," *IEEE Trans. Wireless Commun.*, vol. 4, no. 4, pp. 1407–1411, Jul. 2005.

[23] I. S. Gradshteyn and I. M. Ryzhik, *Table of Integrals, Series, and Products*, 6th ed. New York: Academic, 2000.

[24] A. A. Abu-Dayya and N. C. Beaulieu, "Bandwidth efficient QPSK in cochannel interference and fading," *IEEE Trans. Commun.*, vol. 43, no. 9, pp. 2464–2474, Sep. 1995.

[25] M. Abramovitz and I. A. Stegun, *Handbook of Mathematical Functions With Formulas, Graphs, and Mathematical Tables*, 9th ed. New York: Dover, 1972.

[26] G. K. Karagiannidis, "Performance analysis of SIR-based dual selection diversity over correlated Nakagami-m fading channels," *IEEE Trans. Veh. Technol.*, vol. 52, no. 5, pp. 1207–1216, Sep. 2003.

[27] N. C. Sagias, G. K. Karagiannidis, P. T. Mathiopoulos, and T. A. Tsiftsis, "On the performance analysis of equal-gain diversity receivers over generalized Gamma fading channels," *IEEE Trans. Wireless Commun.*, vol. 5, no. 10, pp. 2967–2975, Oct. 2006.

[28] V. S. Adamchik and O. I. Marichev, "The algorithm for calculating integrals of hypergeometric type functions and its realization in REDUCE system," in *Proc. Int. Conf. Symbolic and Algebraic Comput.*, Tokyo, Japan, 1990, pp. 212–224.

[29] H. Shin and J. H. Lee, "Performance analysis of space-time block codes over keyhole Nakagami-m fading channels," *IEEE Trans. Veh. Technol.*, vol. 53, no. 2, pp. 351–362, Mar. 2004.

[30] A. Papoulis, *Probability, Random Variables, and Stochastic Processes*, 3rd ed. New York: McGraw-Hill, 1991.

[31] S. Sampei, *Applications of Digital Wireless Technologies to Global Wireless Communications*. London, U.K.: Prentice-Hall, 1997.

[32] M.-S. Alouini and A. J. Goldsmith, "Capacity of Rayleigh fading channels under different adaptive transmission and diversity-combining techniques," *IEEE Trans. Veh. Technol.*, vol. 48, no. 4, pp. 1165–1181, Jul. 1999.

[33] T. M. Cover and J. A. Thomas, *Elements of Information Theory*, 1st ed. Hoboken, NJ: Wiley, Sep. 1991.

[34] M.-S. Alouini and A. J. Goldsmith, "Area spectral efficiency of cellular mobile radio systems," *IEEE Trans. Veh. Technol.*, vol. 48, no. 4, pp. 1047–1066, Jul. 1999.

[35] W. C. Y. Lee, "Estimate of channel capacity in Rayleigh fading environment," *IEEE Trans. Veh. Technol.*, vol. 39, no. 3, pp. 187–189, Aug. 1990.

[36] F. Lazarakis, G. S. Tombras, and K. Dangakis, "Average channel capacity in a mobile radio enviroment with Rician statistics," *IEICE Trans. Commun.*, vol. E77-B, no. 7, pp. 971–977, Jul. 1994.

[37] P. Varzakas and G. S. Tombras, "Spectral efficiency for a hybrid DS/FH CDMA system in cellular mobile radio," *IEEE Trans. Veh. Technol.*, vol. 50, no. 6, pp. 1321–1327, Nov. 2001.

[38] R. K. Mallik, M. Z. Win, J. W. Shao, M.-S. Alouini, and A. J. Goldsmith, "Channel capacity of adaptive transmission with maximal ratio combining in correlated Rayleigh fading," *IEEE Trans. Wireless Commun.*, vol. 3, no. 4, pp. 1124–1133, Jul. 2004.

[39] N. C. Sagias, "Capacity of dual-branch selection diversity receivers in correlative Weibull fading," *Eur. Trans. Telecommun.*, vol. 17, no. 1, pp. 37–43, Jan./Feb. 2006.

[40] S. Khatalin and J. P. Fonseka, "Capacity of correlated Nakagami-m fading channels with diversity combining techniques," *IEEE Trans. Veh. Technol.*, vol. 55, no. 1, pp. 142–150, Jan. 2006.

Nikos C. Sagias (S'03–M'05) was born in Athens, Greece, in 1974. He received the B.Sc. degree in physics and the M.Sc. and Ph.D. degrees in telecommunications from the Department of Physics (DoP), University of Athens (UoA), Athens, Greece, in 1998, 2000, and 2005, respectively.

He is currently a Researcher with the Institute of Informatics and Telecommunications, National Centre for Scientific Research—"Demokritos," Athens. In 2000, he was a Research Associate with the Institute for Space Applications and Remote Sensing, National Observatory of Athens, where he participated in several national and European R&D projects. Also, he collaborates with the Laboratory of Electronics, DoP, UoA. He has authored and/or coauthored more than 20 journals and 15 conference papers. His research interests are in the areas of communication and information theory, wireless communication systems (including cellular, satellite and fixed systems), diversity receivers, and fading channels. He also acts as a Reviewer for several international journals and conferences.

Dr. Sagias is a member of the Hellenic Physicists Association. He is the recipient of an Ericsson Award for his Ph.D. thesis.